

# New ways to improve the performance of sealed batteries of high capacity

Yu. Kamenev\*, M. Lushina, N. Chunts, A. Kiselevich, V. Leonov

*Scientific Technical Center ELECTROTYAGA Closed Jointed Stock Company, Saint-Petersburg, Russia*

Received 30 January 2007; received in revised form 30 March 2007; accepted 29 April 2007

Available online 5 May 2007

## Abstract

Herein are considered some ways to improve the performance efficiency of sealed batteries of high capacity by providing uniform electrolyte distribution with battery height, increasing active mass utilization coefficient and limiting PCL effect.

© 2007 Elsevier B.V. All rights reserved.

*Keywords:* VRLA; The AGM-type separator; Double electrodes; Resilient element

## 1. Introduction

Sealed lead batteries are presently widely used in various branches, which can be attributed to their relatively high performance characteristics (capacity, life time), the lowest cost in comparison to other battery types, practically no gassing and minimum maintenance. However, the VRLA battery market analysis shows that the highest capacity reached is 6000 Ah. With that, there is a requirement for operation of these batteries in the horizontal position. This is related mainly to the existing limitation on the height of the AGM-type separator to be equal to approximately 350–400 mm [1,2]. If higher separators are used, the marked distribution of the electrolyte with height occurs, resulting in battery's performance degradation. This work suggests a way to increase the height of the VRLA batteries, which would allow operating them in the conventional vertical position.

Extension of the service life of the lead batteries requires increasing the thickness of the positive current-carrying electrode, which is connected with a certain rate of its corrosion. According to data in Ref. [3], the corrosion rate of the lead alloys is about 0.05 mm per year at 25°C and a charging voltage of 2.25 V. The practice demonstrates that service lives of 5, 10 and 15 years are provided by positive electrodes with a thickness correspondingly 2.5–3.0, 3.5–4.0 and 4.5–5.0 mm [4]. However, the use of thicker electrodes results in decrease in the active mass

utilization coefficient. This work suggests a way to improve the performance efficiency of thicker positive electrodes.

The efficient performance of the VRLA batteries with the AGM-type separator requires constant compression of the electrode package, which allows to exclude adverse impact of PCL-2 effect. PCL-2 effect is a loss of electrical conductivity in the active mass due to progressive expansion of the positive active mass during cycling [15]. However, in the process of battery operation, the AGM-type separator loses its elastic properties [5]. This work suggests a method allowing to provide a specified rate of compression of the electrode package during the whole cycling period of the VRLA batteries.

## 2. Experimental results and argumentation

### 2.1. Zero porosity zones in the AGM separators

In work [6], we have investigated the stationary distribution of the electrolyte in a 900 mm high AGM separator while exposed to the gravitational field, and studied electrolyte distribution factors. It has been shown that increase in separator compression rate contributes to increase in electrolyte distribution with the height of the separator. However, one-side compression leads to a decrease in the separator porosity and, consequently, to a decrease of its electrolyte volume. But, on the other hand, it contributes to diminishing of the radius of the separator pores and increasing pressure required to create gas channels providing fast transport of oxygen from positive to negative electrode. Therefore, separator compression cannot be regarded as a way of providing a uniform distribution of the electrolyte with the height

\* Corresponding author. Tel.: +7 812 3169643; fax: +7 812 786 97 19.  
E-mail address: [lushina@mail.wplus.net](mailto:lushina@mail.wplus.net) (Yu. Kamenev).

of a high-capacity VRLA separator operating in the vertical position.

In work [7], we have investigated the height and velocity of capillary rise of the electrolyte in an AGM separator, and impact of different factors (separator compression rate, acid concentration) on the process. The electrolyte rise ( $H$ ) can be determined by the following expressions:

$$F_C = F_g \quad (1)$$

$$H = \frac{2\gamma \cos\theta}{\rho\beta Rg} \quad (2)$$

where  $F_C$  is the capillary force,  $F_g$  the gravitational force,  $\gamma$  the surface tension,  $\theta$  the contact angle,  $\rho$  the density of electrolyte,  $\beta$  the pore tortuosity factor,  $R$  the pore radius and  $g$  is the gravitational constant.

It has been shown that if no compression is applied to the separator, electrolyte rise comes to 400 mm at an electrolyte density of  $1.05 \text{ g cm}^{-3}$  and 200 mm at  $1.28 \text{ g cm}^{-3}$ . By increasing the separator compression rate by 30%, the figures are correspondingly 500 and 350–400 mm. Thus, it has been proved once again that stable distribution of the electrolyte in high VRLA batteries (above 400–500 mm) cannot be achieved by separator compression.

This work suggests a new way of providing a uniform distribution of the electrolyte with height by creation of zero porosity zones in the AGM separators. The core of the method is that thin zero porosity strips are formed across the full width of the separator by impregnating it with different compositions. Such strips are called zero porosity zones (ZPZ) and are formed across the height of the separator at 300–350 mm intervals (Fig. 1), i.e. at intervals equal to the capillary rise of the electrolyte in the AGM separator. ZPZ width is 1.0–3.0 mm. It is obvious that the presence of ZPZ should prevent the electrolyte from flowing down the separator and provide due to this its uniform distribution with height.

Zero porosity zones have been formed using compositions of different polymeric materials (natural rubber, perchlorovinyl, styrene acrylonitrile and others), dissolved in different organic solvents (acetone, toluene and others). Compositions with different fluidities have been obtained by changing the component ratio. Also, different technologies of formation of ZPZ have been applied. Both separator impregnation methods and methods of gluing together its parts have been changed.

The created zero porosity zones have been tested for electrolyte impermeability by applying the following procedure. A 100 mm wide AGM-separator plate with a transverse ZPZ was fixed in the vertical position so that one of its ends was dipped in a colored solution of  $\text{H}_2\text{SO}_4$  with a density of  $1.28 \text{ g cm}^{-3}$ , with the ZPZ having been positioned in parallel with and at 2–3 cm from the solution surface. With occurrence of gravitational forces the capillary rise height in AGM separator is far above 2–3 cm. The separator with the ZPZ was held in such position maximum for a year. If the ZPZ did not have sufficient quality, the electrolyte quickly penetrated through it, and the separator's area above the ZPZ got colored. On the other hand, if a ZPZ material was not acid resistant, the ZPZ lost its impermeability in

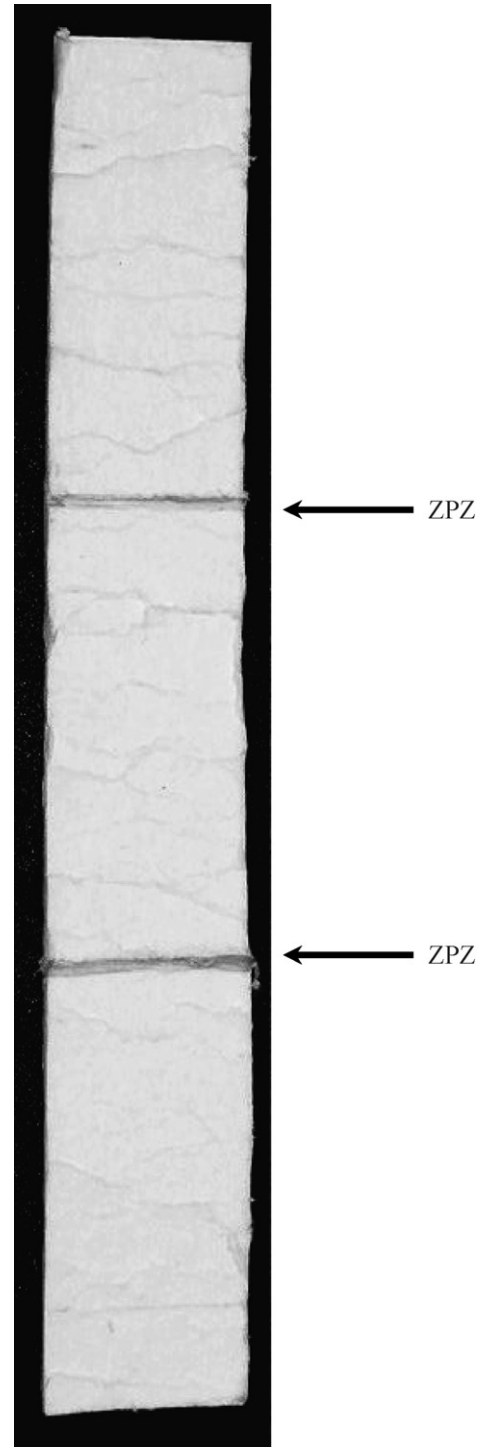


Fig. 1. AGM-type separator with zero porosity zones (a width of ZPZ is 5–7 mm).

some time. Selection of materials and application technologies made it possible to obtain a ZPZ preventing electrolyte penetration (no coloring of the separator area above ZPZ) for a year.

A ZPZ efficiency utilization test has been carried out according to the procedure set out in Ref. [2]. One hundred millimeter wide 900-mm high AGM-separator plates with one ZPZ arranged at a height of 450 mm and two ZPZ at heights of 300 and 600 mm were placed between vinyl plates with a fixed gap

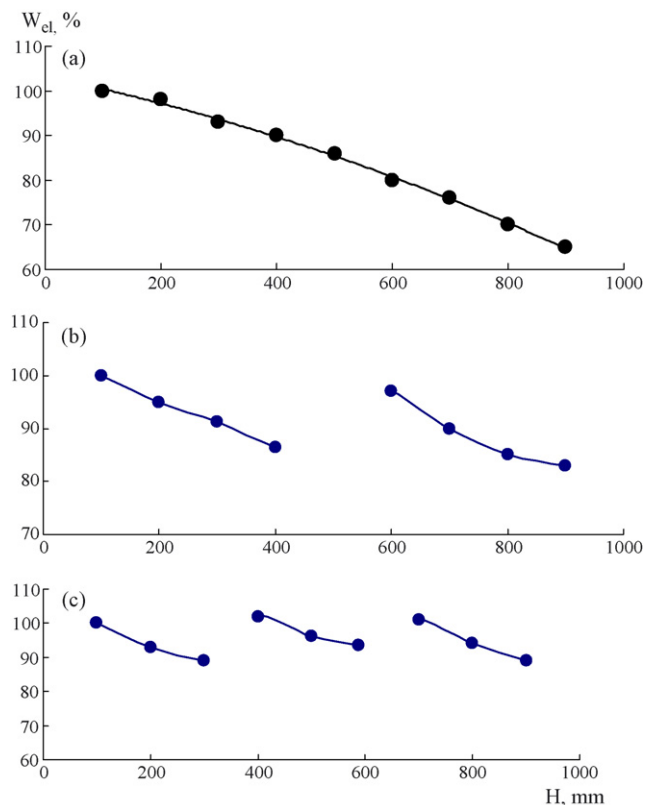


Fig. 2. Electrolyte distribution ( $W_{el}$ , %) with separator height ( $H$ , mm): without ZPZ (a), with one ZPZ (b) and two ZPZs (c).

between them. After placing the separator in the gap, the plates were clamped together uniformly and fixed. The unit thus assembled was placed into a horizontal container with electrolyte, and the separator was impregnated for 3 days. After the impregnation treatment the unit was set vertically into a cylinder, and the whole arrangement was sealed with a polyethylene cover to avoid electrolyte losses due to its evaporation. The unit was held in the vertical position for 14 days. On completion of the period, the unit was disassembled in the vertical position, and separator plate was cut into 50 mm pieces, every piece was placed in a preliminary weighted glass, which were then weighted with an accuracy of  $\pm 0.01$  g to determine the electrolyte content. Then the pieces of separator were washed, dried and weighted once more for determining the separator weight without electrolyte. On the basis of the weighting results a curve of electrolyte distribution versus separator height was plotted. Experiments with similar separator plate without ZPZ were carried to for comparison purposes.

Experimental results are shown in Fig. 2. It can be seen in the figure that the presence of ZPZ substantially improves the uniform electrolyte distribution with separator height due to a significant slowdown of the electrolyte flowing down process caused by the gravitational force. For example, without ZPZ, the ununiformity factor, defined as the ratio between the electrolyte interpenetration at a height of 850–900 mm to electrolyte interpenetration at a height of 0–50 mm, is in this case approximately 0.65. With ZPZ, the ununiformity factor is 0.80, and with two ZPZ—0.95.

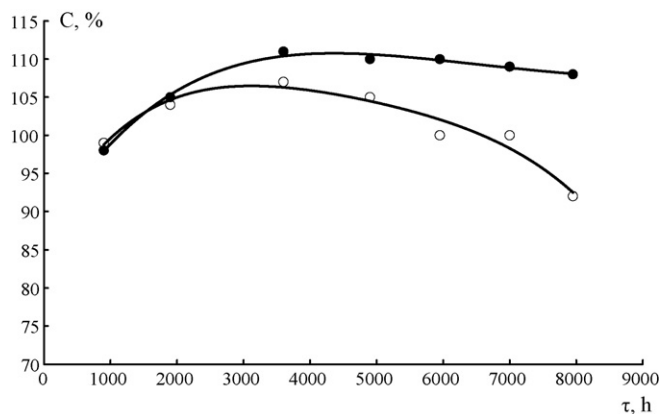


Fig. 3. Battery capacity change as percentage of the rated capacity in the course of testing: (●) batteries with ZPZ, (○) batteries without ZPZ.

Thereby was demonstrated the efficiency of ZPZ utilization to provide stable electrolyte retention in the separators of high-capacity VRLA batteries with a significant height dimension.

The problem is that a gap between the ZPZ and the electrodes will allow redistribution of the electrolyte. ZPZ efficiency was checked for practicable batteries.

Two versions of batteries with a rated capacity of 800 Ah at 20-h discharge were assembled. The height of the separator of such batteries was 680 mm. The batteries of one version had separators without ZPZ, the batteries of the other version were with one ZPZ at a height of 340 mm, that is the ZPZ divided the separator into two equal portions. The batteries were tested in thermostatic containers at  $50^\circ\text{C}$ . The test program included alternating continuous float charge periods with a duration of approximately 1000–1500 h at a battery voltage of 2.25 V and test discharges with 20-h discharge current. The test discharges were carried out at  $20\text{--}25^\circ\text{C}$ .

Fig. 3 shows the relationship between the capacity of 20-h test discharges and continuous float charge test time. It can be seen in the figure that batteries with separators with ZPZ are distinguished by stable characteristics due to their uniform electrolyte distribution. For example, after eight continuous float charge periods the capacity of the batteries with ZPZ practically did not change, whereas the batteries without ZPZ reduced their capacity by on average 8–10%.

## 2.2. Double electrodes

To extend service life (up to 10 years and longer), thick positive grids, capable to maintain their required mechanical properties after a long simultaneous exposure to high anode potential, aggressive environment and heat, are used. Practice shows that the thickness of the grids of the batteries with service lives of 10 and 15–20 years must be correspondingly 3.0–3.8 and 4.5–5.0 mm. For instance, with a 15–20-year service life guarantee, the companies YUASA and EXIDE use positive grids with 4.7 mm thickness; the company GNB, 4.9 mm; the company EAST PENN, 5.2 mm; the company C&D, 6.0 mm [4,8]. In addition, the above companies use alloys with increased corrosion resistance. The corrosion rate of the alloys is normally

0.05 mm year<sup>-1</sup> [3]. Consequently, the 5.0 mm original thickness of the grid would reduce to 3.0 mm after 20-year operation. Therefore, thick electrodes are required to be used, but increase in their thickness leads to decrease in the active mass utilization coefficient as acid diffusion into the depth of the electrode is hindered.

The point of the technical solution suggested by this work is to have two thin electrodes with a common conductor lug spaced with a glass fiber separator. At that, the total two-electrode system thickness must be equal to the thickness of one electrode. In this case acid diffusion channel would be substantially shortened, and increase in the active mass utilization coefficient should be expected. This should made a major impact for positive electrodes as the diameter of their pores is much less than that of the negative electrode. For example, according to data in Ref. [9], the average diameter of the pores of the positive active mass is 0.3–0.5 μm and negative, 1.0–1.5 μm.

It is common knowledge that the corrosion rate of the grids highly depends on the value of their polarization [10]. It is obvious that the current through an individual grid in a double system will, with current redistribution not taken into account, be twice as less as that through a thick grid. In such case, the polarization level will become significantly reduced and, correspondingly, corrosion rate as well. The strong dependence of a grid corrosion (acceleration factor (*k*)) from positive plate polarization (ppp) was denoted in work [3], of which follows that at ppp equal to 100, 200 and 300 mV, the factor *k* is 1, 2.3 and 5, respectively. Therefore, simultaneous reduction in the thickness of the electrodes and their corrosion rate can ensure the performance of the double system at the level of thick electrode performance.

This work includes the tests of the efficiency of double electrodes as positive and negative battery plates.

Two electrode types were manufactured. One of the electrode type was manufactured by applying the following procedure. Two grids (3.6 mm thick 190 mm × 131 mm) were welded along the frame perimeter and after its was pasted as a single grid. The pasting done from both sides. Then forming was carried out in 1.07 g cm<sup>-3</sup> acid by 0.7 A dm<sup>-2</sup> current. The thickness of such electrode was 7.2–7.3 mm. To manufacture the other electrode type, two formed similar 3.6 mm thick electrodes were taken. They were spaced with a AGM separator with a thickness of 1.1 mm and welded together. A separator compression rate in the double electrode was 40–50%. The total thickness of the double electrode was, on average, 7.3 mm. The active mass content in

the double electrodes and thick electrodes was much the same. In comparing the discharge capacity characteristics of two types of electrodes the specific values were used (ampere hour per kilogram).

Both positive and negative electrodes of both types were manufactured.

Then battery mock-ups of the following versions were assembled:

- one thick positive electrode in the centre and two outside negative electrodes (version 1);
- one double positive electrode in the centre and two outside negative electrodes (version 2);
- one thick negative electrode in the centre and two outside positive electrodes (version 3);
- one double negative electrode in the centre and two outside positive electrodes (version 4).

The electrodes of the opposite polarity were spaced with 2.8 mm thick AGM separators. A separator compression rate in the package was 20%. The mock-ups were filled with 1.28 g cm<sup>-3</sup> acid. The active mass quantity in the outside electrodes was two times more than that in the central electrodes. During cycling the capacity of the mock-ups was limited to the capacity of the central electrodes.

In total, three mock-ups of each version had been assembled. All outside electrodes had a substantial excessive active mass, which excluded their impact on the discharge capacity of the mock-ups.

After filling with acid, the mock-ups were subjected to cycling including a two-stage charging with a first stage current of 6 A up to a voltage of 2.40 V and a second stage current of 3 A with limited overcharge (5%), and discharging with *C*<sub>20</sub> current to an end point voltage. Test discharges with *C*<sub>20</sub> current up to an end-point voltage of 1.75 V and *C*<sub>5</sub> current up to an end-point voltage of 1.70 V were carried out in succession every 10 cycles.

In Tables 1 and 2 are given changes in capacity per unit of active mass weight during cycling for 20- and 5-h discharge rates. The 10th cycle capacity was taken as the rated specific capacity. Average test values of the three mock-up types are given in the tables.

Fig. 4a shows the efficiency of double and thick electrodes versus the number of cycles at 20-h discharge rate, and Fig. 4b

Table 1  
Specific capacity of battery mock-ups at 20-h discharge rate

Cycle number	Specific capacity at 20-h discharge rate (Ah kg <sup>-1</sup> )			
	Positive electrode		Negative electrode	
	Thick electrode	Double electrode	Thick electrode	Double electrode
10	89.6	119.2	165.0	165.6
20	98.5	123.9	158.1	169.2
40	105.6	126.6	163.8	171.6
50	105.6	120.7	165.6	171.0
68	98.9	112.6	170.3	172.8
90	87.2	94.4	168.4	168.8

Table 2  
Specific capacity of battery mock-ups at 5-h discharge rate

Cycle number	Specific capacity at 5-h discharge rate (Ah kg <sup>-1</sup> )			
	Positive electrode		Negative electrode	
	Thick electrode	Double electrode	Thick electrode	Double electrode
31	66.7	98.9	141.4	160.3
45	69.4	100.4	151.0	158.4
52	66.2	98.3	149.0	155.1
71	58.6	87.5	153.4	156.1
91	60.6	81.0	150.8	154.0
108	60.3	74.3	151.4	150.8

shows the similar relationship at 5-h discharge rate. The efficiency is defined as a ratio of capacity difference of double and thick electrodes to the capacity of a thick electrode, in percent. It follows from the figures that the efficiency of double positive electrodes at 20-h discharge rate ( $E_{(+20)}$ ) has maximum value, 33%, at initial cycles and gradually declines as cycling goes. At the 90th cycle  $E_{(+20)}$  is 8.3%. The efficiency of double negative electrodes ( $E_{(-20)}$ ) has the same qualitative nature, but substantially lower level. For instance, at the 20th cycle  $E_{(-20)}$  equals to 7.0%, and at the 90th cycle just 0.4%. The efficiency of double positive electrodes at 5-h discharge rate ( $E_{(+5)}$ ) is higher than that at 20-h discharge rate, and it is stable in a cycling range of 0–70 cycles.  $E_{(+5)}$  is 42–50% in this range. Then the efficiency declines and comes to 23.2% before the 107th cycle. The efficiency of double negative electrodes ( $E_{(-5)}$ ) is also higher than in the case of 20-h discharge rate. For instance, it is 13.4% at the 31st cycle and comes to 0 before the 108th.

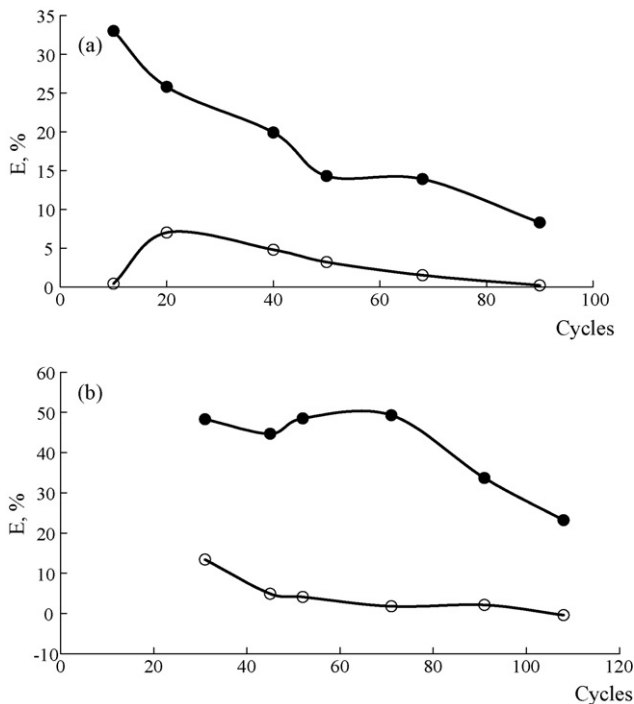


Fig. 4. Change in efficiency of utilization ( $E$ , %) of double positive (●) and negative (○) electrodes in the course of cycling at 20-h (a) and 5-h discharges (b).

The indicated facts: (1)  $E_{(+5)} > E_{(+20)}$ ; (2)  $E_{(-5)} > E_{(-20)}$ ; (3)  $E_{(+20)} > E_{(-20)}$ ; (4)  $E_{(+5)} > E_{(-5)}$  can be explained by applying the following process model.

Let us consider a porous system of electrodes as a system of cylinder pores with effective radius  $r$  and tortuosity  $\beta$ . On the one hand, acid concentration decreases during discharging due to a current generation process, on the other hand it increases as a result of acid diffusion transfer. Now, the amount of the acid in a pore with the radius  $r$  at the distance  $d/2$ , where  $d$  is electrode thickness, from the surface of the electrode will change in the time  $\tau$  by the value  $\delta m$  equal to

$$-\delta m = \delta m_i - \delta m_D$$

$$-\delta m = m_0 - m_\tau = k_1 \times I_P \times \tau - \frac{2Ds}{\beta d}(C_0 - \bar{C})\tau \quad (3)$$

where  $\delta m_i$  is the reduction in acid amount due to charge transfer reaction;  $\delta m_D$  the increase in acid amount due to diffusion processes;  $m_0$ ,  $m_\tau$  the acid increase in specified volume at the time 0,  $\tau$  correspondingly;  $k_1$  the discharge current share  $I_P$  in specified volume;  $D$  the diffusion coefficient;  $s = \pi r^2$  the average cross-section of pores;  $C_0$  the acid concentration in electrode pores at the time 0 and in electrolyte volume;  $C$  is the effective concentration in the time interval (0,  $\tau$ ). As a first approximation it can be assumed that  $C = (C_0 + C_\tau)/2$ , then

$$\Delta m = m_0 - m_\tau = k_1 \times I_P \times \tau - \frac{Ds}{\beta d}(C_0 - C_\tau)\tau \quad (4)$$

where  $C_\tau$  is the acid concentration at the time  $\tau$ . By substituting masses by concentrations and taking into account that  $s = \pi r^2$ , the following is obtained

$$C_0 - C_\tau = \frac{k_1 I_P \tau}{\pi r^3} - \frac{D\tau}{\beta dr}(C_0 - C_\tau) \quad (5)$$

Solving (3) relative to  $C_\tau$ , the following is obtained

$$C_\tau = C_0 - \frac{k_1 I_P}{\pi r^2(r/\tau + D/\beta d)} \quad (6)$$

It follows from (6) that the thicker electrode ( $d$ ), the lower acid concentration in the pores of deep electrode layers during discharging ( $C_\tau$ ), which follows from the limited rate of its diffusion into the depth of the electrode. Consequently, the use of thin double electrodes should contribute to increase the amount of acid

in inner layers and improve the performance efficiency of the electrodes.

It is particular important in case of intensive discharges when acid consumption grows substantially and diffusion rate is not enough to compensate its outflow. Different performance efficiencies of the positive and negative electrodes can be related to their different pore diameters. It follows from (6) that pore radius increase leads to increase of  $C_\tau$ , which is related to the increase in the rate of diffusion into the depth of the electrode. It is known that average radius of the negative active mass is much more than that of the positive active mass and, consequently, the utilization efficiency of the double system for negative electrodes should be less. That was observed during testing. The decline in the utilization efficiency of the double electrodes in the course of cycling is attributed to the fact that in time current generation processes are forced out into surface layers of the electrodes, and the difference between their  $d$  values is becoming lesser.

### 2.3. Resilient element

The main cause of the lead battery failure is known to be the loss of contact between its active mass and current-carrying electrode due to volumetric changes in the course of cycling (PCL-2 effect) [10]. The PCL-2 effect can also be facilitated by the growth of the positive electrode caused by the wedging action of corrosion products produced along grain boundaries [11,12]. One of the effective ways of limiting PCL-2 effect (AM shedding) is compression of the electrode package [13–15]. With that, the separator prevents active mass from expansion. Such compression can be easily implemented in sealed batteries where an AGM with high elasticity and tightly fit plate surface is used as a separator. However, it should be clear that package compression has its negative effects associated with decrease in the average radius of the pores of the compressed separator. In such a case, on the one hand, it hinders creation of gas channels in the separator due to increase in resistance to force electrolyte out of the pores by the oxygen produced on the positive electrode. But on the other hand, the compressed separator's pore radius becomes comparable with that of the negative AM pores, which can lead to undesirable redistribution of the electrolyte between the separator and negative electrode. It is common knowledge that the average radius of the negative AM pores is 1–5  $\mu\text{m}$ , and that of the pores of an uncompressed glass felt separator is 5–15  $\mu\text{m}$  [9]. A 30–40 kPa compressed separator has the average radius of pores 0.8–1.5  $\mu\text{m}$  [9], i.e. the dimension comparable with the radius of the negative active mass pores. Consequently, the optimization of the separator compression rate should be carried out both with respect to the period of service parameter and oxygen cycle efficiency. Besides, initially set compression in the package can change in the course of battery cycling. This is connected both with a decrease in resilience of the glass felt separator due to electrode thickness variation and a change in the separator thickness due to a reduction in its electrolyte filling caused by electrolyte losses. Therefore, it is important not only to determine the optimal package compression rate, but also to maintain it during battery's service life.

Sealed batteries with a rated capacity of 15 Ah and electrode package initial compression rates of 3–5%, 22–25%, 38–40% and 55–57% (three batteries with each compression rate) were manufactured. The initial compression rate was provided by placing different number of separator layers in the interelectrode gaps and changing the value of interelectrode gap in the batteries. The separator thickness is 2.03 mm (at 10 kPa). The initial compression rate equal to  $(1 - d/n\delta) \times 100\%$ , where  $d$  is the interelectrode gap,  $\delta$  the thickness of separator,  $n$  is the number of separator layers. The batteries were filled with 1.28  $\text{g cm}^{-3}$  acid and subjected to cycling at room temperature by applying the following procedure: a two-stage charging with a first stage current of 2 A up to a voltage of 2.40 V and a second stage current of 0.2 A with limited overcharge (15%) and discharging with current  $C_5$  for 4 h. Two test discharges at 20-h discharge current to an end-point voltage of 1.75 V and at 5-h discharge current to an end-point voltage of 1.66 V were conducted every 20 cycles. Also, the battery were weighted every two to three cycles to determine electrolyte losses and oxygen cycle efficiency.

Fig. 5 shows the cycling results for the batteries with different rates of electrode package compression. It can be seen that the discharge capacity and battery service life-compression rate relationship is of extreme nature, with the maximum within a range of 25–40%. Evidently, the required degree of contact of the separator with the electrodes to exclude the PCL-2 process is not provided at low package compression. Changes in separator structure (porosity, pore radius) play negative role at too high compression. Moreover, at high compression rate, the AGM separator can lose its elastic properties due to irreversible damage to its fiber. The battery weight losses giving an indication of the oxygen cycle efficiency (total water losses)–electrode package compression rate relationship (Fig. 5) is also of extreme

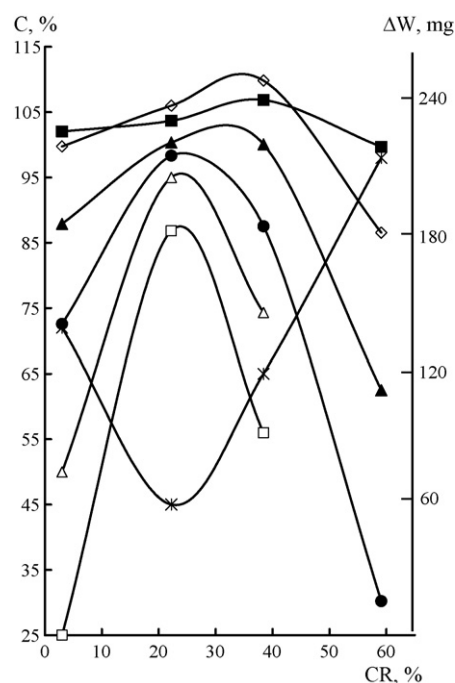


Fig. 5. Capacity ( $C$ , %) and total weight losses of the batteries ( $\Delta W$ , mg)–electrode package compression rate (CR, %) relationship. Cycle number: 33 (■), 75 (◇), 94 (▲), 114 (●), 134 (△), 154 (□);  $\Delta W$  (mg) (✕).

nature, with the minimum within a range of 20–25%. It can be believed that poor contact between the separator and electrodes takes place at low compression rate, which leads to increase in the thickness of liquid layer at the positive electrode-separator and negative electrode-separator boundaries, and to increase in water losses during charging process due to substantial reduction in the oxygen transfer rate, according to the well-known Fick equation. At high compression rates, the substantial decrease in the separator pore radius hinders during charging process the creation of gas channels required to transport oxygen and establish efficient oxygen cycle, which leads to increase in battery water losses. Therefore, the optimum package compression rate should be considered 20–30%. The obtained results comply with Refs. [13,16].

To provide the stability of the specified compression rate and thickness variation compensation during service life, it has been suggested to use additional resilient elements in the gap between the electrode package (its front surface) and container wall. This work sets out tests of a VRLA battery with a rated capacity of 350 Ah provided with resilient elements. A system of a thin vinyl plate adjacent to the electrode and spiral taper washers glued to the container wall surface (Bellewill washers) was used as a resilient element. The Bellewill washers' special feature is that the higher rate of their compression, the higher pressure they exert on the electrode package. Work [17] suggests to use another system of resilient elements.

Battery tests have been carried in thermal chambers in an accelerated mode at 50 °C. The batteries have been held at a stable voltage of 2.25 V for 1000 h and then 20-h test discharges have been carried out at 20 °C. The total operating time of the batteries at 50 °C was 22,000 h. At that, the capacity of the batteries with resilient elements dropped by 7.5–8.0%, whereas the capacity of the reference batteries without resilient elements dropped by 16–20%.

### 3. Conclusion

1. The work demonstrates the efficiency of utilization of zero porosity zones in the AGM separator for vertically operated high-capacity VRLA batteries. It has been shown that the presence of such zones allows to provide uniform electrolyte distribution for a 900 mm high separator.
2. It has been shown that replacement of one thick electrode with a double positive electrode allows to substantially increase the positive active mass utilization coefficient. The use of double negative electrodes has a restricted effect.
3. It has been shown that the use of resilient elements providing optimal electrode package compression rate during cycling makes it possible to extend VRLA battery service life.

### References

- [1] G. Zguris, *J. Power Sources* 88 (2000) 36–43.
- [2] B. Culpin, *J. Power Sources* 53 (1995) 127–135.
- [3] S.L. Vechy, Absolyte Technology, Professional Papers, GNB Industrial Battery Company, GB-3819, REV 9/98, pp. 4.1–4.9.
- [4] L.S. Holden, *J. Power Sources* 59 (1996) 115–118.
- [5] K. Sawai, M. Shiomi, Y. Okada, *J. Power Sources* 78 (1999) 46–53.
- [6] Y. Kamenev, A. Kiselevich, E. Ostapenko, *J. Power Sources* 102 (2001) 218–223.
- [7] Y. Kamenev, M. Lushina, E. Ostapenko, *J. Power Sources* 109 (2002) 276–280.
- [8] L.S. Holden, *Power Qual. Assurance Mag.* 1–2 (2000) 1–4.
- [9] B. Nelson, *Batteries Int.* (April) (2000) 51–60.
- [10] D. Berndt, *J. Power Sources* 95 (2001) 2–12.
- [11] D. Pavlov, *J. Power Sources* 53 (1995) 9–21.
- [12] R.D. Prengaman, *Battery Man.* (April) (1997) 23–31.
- [13] G. Zguris, *J. Power Sources* 73 (1998) 60–64.
- [14] W. Böhnstedt, *J. Power Sources* 78 (1999) 35–40.
- [15] C. Pendry, *J. Power Sources* 78 (1999) 54–64.
- [16] G. Zguris, *Battery Man.* (August) (1997) 28–31.
- [17] M. Weighall, *Batteries Int.* (January) (2001) 53–58.